

# Convolutional Neural Network Compression Based on Low-Rank Decomposition

Yaping He  
College of Computer and Information  
Science College,  
Southwest University,  
Chongqing, China  
yapinghe93@gmail.com

Linhao Jiang  
Shapingba Community Health  
Service Center,  
Shapingba District,  
Chongqing, China  
18333140@qq.com

Di Wu  
College of Computer and Information  
Science College,  
Southwest University,  
Chongqing, China  
wudi.cigit@gmail.com

**Abstract**—Deep neural networks typically impose significant computational loads and memory consumption. Moreover, the large parameters pose constraints on deploying the model on edge devices such as embedded systems. Tensor decomposition offers a clear advantage in compressing large-scale weight tensors. Nevertheless, direct utilization of low-rank decomposition typically leads to significant accuracy loss. This paper proposes a model compression method that integrates Variational Bayesian Matrix Factorization (VBMF) with orthogonal regularization. Initially, the model undergoes over-parameterization and training, with orthogonal regularization applied to enhance its likelihood of achieving the accuracy of the original model. Secondly, VBMF is employed to estimate the rank of the weight tensor at each layer. Our framework is sufficiently general to apply to other convolutional neural networks and easily adaptable to incorporate other tensor decomposition methods. Experimental results show that for both high and low compression ratios, our compression model exhibits advanced performance.

**Keywords**—*model compression, deep neural networks, orthogonal regularization, VBMF, edge devices.*

## I. INTRODUCTION

Given the rapid development of artificial intelligence technology [1]-[10], deep neural networks have achieved great success. They have been widely used in tasks such as image classification [11], object detection [12], and so on. Nevertheless, executing DNNs in embedded devices is still challenging. Many of the resource-constrained devices face the challenge that advanced DNNs have parameter sizes too large for real-world deployment. This limitation hinders the practical deployment of the models. In response to this challenge, numerous researchers have proposed various types of strategies to lightweight models and reduce model parameters.

**Tensor Decomposition for Model Compression.** Tensor decomposition [13]-[20] offers significant advantages in managing large-scale tensor data [20]-[26] owing to its favorable mathematical properties. As such, tensor decomposition has emerged as an exceedingly appealing technique for model compression. It can offer exceptionally high compression ratios for models with minimal performance degradation compared to other compression schemes [1]. In particular, for recurrent neural networks [27][28], state-of-the-art tensor decomposition methods can achieve thousands of times parameter compression, while significantly enhancing accuracy. Driven by the impressive compression performance, an increasing number of researchers are investigating model compression [29][30] methods rooted in tensor decomposition.

**Limitations of prior art.** Despite the maturity of tensor decomposition techniques and the satisfactory results obtained, there are limitations. Parametric compression achieving thousands of times reduction is only prevalent in video compression tasks. In the case of Convolutional Neural Networks (CNNs) employed in image categorization tasks, performance severely deteriorates, even with state-of-the-art Tensor Train (TT) and Tensor Ring (TR) decompositions. For instance, despite leveraging the latest advances in TR, a 1.0% decrease in accuracy persists with a compression ratio of 2.7 for the ResNet-32 model on the CIFAR-10 dataset. With a larger compression ratio of 5.8, the accuracy loss escalates to 1.9% [24].

**What limits performance?** Tensor decomposition suffers from the above limitations mainly due to the model's lack of robustness and the choice of rank. Specifically, tensor decomposition typically breaks down a layer of a neural network into multiple consecutive sublayers, and the resulting factor matrix often adheres to specific mathematical forms, such as orthogonality [32][33]. However, the factor matrix, representing the weight matrix of the compressed neural network's sublayers, gets updated during each iteration, making it challenging to satisfy the initial mathematical properties. Additionally, a significant imbalance exists between the input and output channels in the neural network, rendering decomposing different modalities using the same rank highly unreasonable [34]. In short, these two aforementioned factors can significantly compromise the model's performance.

**Technical Preview and Contributions.** To address these limitations, our paper introduces a model compression method that integrates orthogonal regularization and VBMF. Initially, the model undergoes training with over-parameterization while imposing orthogonal regularization simultaneously, ensuring it achieves or exceeds the accuracy of the original model. Subsequently, VBMF

is utilized to estimate the tensor rank for each layer of the neural network. Finally, low-rank training is conducted, leading to the acquisition of the compressed model. In summary, the contributions of this paper are outlined as follows:

- We propose a framework for addressing the model compression problem. By conducting training with over-parameterization and orthogonal regularization, not only are better initial values provided for low-rank models, but also orthogonal properties are obtained.
- We employ the VBMF method to estimate the rank of one modality in the TK-2 decomposition, while the other modality is addressed through the relationship among the input and output channels of the convolutional neural network.
- The proposed framework is evaluated across various DNN models employed in image classification. Experimental results show that for both high and low compression ratios, our compression model exhibits advanced performance.

## II. RELATED WORK ON DNN MODEL COMPRESSION

### A. Sparsification

Sparsification usually refers to reducing the number of model parameters in machine learning and computer vision to improve the efficiency and performance of the model. In deep learning, sparsification techniques[35]-[42] can help reduce the complexity of the model, lowering memory and computational requirements while potentially improving the generalization of the model. Different levels of network structures can be sparse, such as weights, filters, and channels. To obtain sparsity, models can be trained with pruning or sparse perceptual regularization. Sparsification can also be classified as structured [43] and unstructured [44]. Unstructured models usually have high accuracy and compression ratios, but this approach is not friendly to embedded platforms due to irregular memory accesses and unbalanced workloads [45][46]. Structured sparse models are more adapted to hardware deployments, however their compression performance is usually not as good as the same type of unstructured models.

### B. Tensor Decomposition

Tensor decomposition is a widely used technique in machine learning and data science that simplifies models and reduces computational complexity by decomposing higher-order tensors into products of lower-order tensors. Truncated singular value decomposition (TSVD) has good performance in decomposing matrices, however, compared to other tensor decomposition methods such as Tucker [47], and CANDECOMP/PARAFAC (CP) decomposition [48], TSVD [49] is slightly weak when dealing with higher order tensors, which can result in severe loss of accuracy with limited compression ratio. With the development of tensor network technology, TT [50]-[55], and TR decomposition have become the mainstream of compression methods. Due to their unique structural properties, they can give the model an extremely high compression ratio. These advantages are more obvious in RNN networks for video tasks. TT and TR are used to decompose the network input and hidden layers, and it is even able to compress the network tens of thousands of times in some special networks. However, TT [50] and TR [56] perform poorly in some CNNs and cause severe accuracy loss even with a small compression ratio. From a practical application point of view, this non-negligible accuracy loss limits the wide use of the model in embedded devices.

### C. Rank Selection

Tensor decomposition techniques can significantly reduce the number of parameters and computational complexity of a model by decomposing a high-dimensional tensor into a sum of low-rank tensors when compressing a neural network model [58]-[62]. Selecting the optimal rank is the key to achieving effective compression, which requires a balance between model accuracy and computational efficiency. Auto-ML methods [63], automated techniques based on parameter estimation and genetic algorithms [64]-[67], and variational Bayesian [68]-[70] matrix decomposition have been proposed to automate the selection of the optimal rank. In addition, the practice involves manually adjusting and experimenting with different rank choices, as well as approximating matrices using techniques such as TSVD. Together, these methods have contributed to the application and development of tensor decomposition techniques in deep-learning model compression.

## III. MODEL COMPRESSION METHOD

### A. Low-rank Tucker representation of Convolutional layers

In CNNs, Convolutional layers map an input tensor  $\mathbf{X} \in \mathbb{R}^{S \times W \times H}$  into an output tensor  $\mathbf{Y} \in \mathbb{R}^{T \times W' \times H'}$  with a four-order kernel tensor  $\mathbf{K} \in \mathbb{R}^{D \times D \times S \times T}$ . Convolutional computation represents a linear mapping. And it is defined as [47]:

$$\mathbf{Y}(w', h', t) = \sum_{i=1}^D \sum_{j=1}^D \sum_{s=1}^S \mathbf{K}_{i,j,s,t} \mathbf{X}_{h_i, w_j, s}, \quad (1)$$

$$h_i = (h' - 1)\Delta + i - P \text{ and } w_j = (w' - 1)\Delta + j - P,$$

where the size of  $\mathbf{K}$  is  $D \times D \times S \times T$ ,  $\Delta$  and  $P$  represent stride and zero-padding size, respectively.

TK decomposition has unique advantages in CNNs, so we will use TK decomposition to decompose the convolutional layers in this paper. The decomposition process is as follows:

$$K_{i,j,s,t} = \sum_{r_1=1}^{R_1} \sum_{r_2=1}^{R_2} \sum_{r_3=1}^{R_3} \sum_{r_4=1}^{R_4} \mathbf{G}_{r_1,r_2,r_3,r_4} \mathbf{U}_{i,r_1}^{(1)} \mathbf{U}_{j,r_2}^{(2)} \mathbf{U}_{s,r_3}^{(3)} \mathbf{U}_{t,r_4}^{(4)}, \quad (2)$$

where  $\mathbf{G} \in \mathbb{R}^{R_1 \times R_2 \times R_3 \times R_4}$  is core tensor,  $\mathbf{U}^{(1)} \in \mathbb{R}^{D \times R_1}$ ,  $\mathbf{U}^{(2)} \in \mathbb{R}^{D \times R_2}$ ,  $\mathbf{U}^{(3)} \in \mathbb{R}^{S \times R_3}$  and  $\mathbf{U}^{(4)} \in \mathbb{R}^{T \times R_4}$  are factor matrices.

In TK decomposition, not every mode needs to be decomposed. For example, weight  $\mathbf{K}$  can retain mode-1 and mode-2 because the size of the convolution kernel will usually be small, such as  $3 \times 3$  or  $5 \times 5$ . Thus, the weight tensor can be expressed as follows:

$$K_{i,j,s,t} = \sum_{r_3=1}^{R_3} \sum_{r_4=1}^{R_4} \mathbf{G}_{i,j,r_3,r_4} \mathbf{U}_{s,r_3}^{(3)} \mathbf{U}_{t,r_4}^{(4)}, \quad (3)$$

where  $\mathbf{G} \in \mathbb{R}^{D \times D \times R_3 \times R_4}$  is a core tensor. This method is known as TK-2 decomposition. Considering the advantages of convolutional operations in terms of parallelism, etc., we reconstruct the factor matrix into three consecutive convolutional layers in this paper.

$$\mathbf{Z}_{h,w,r_3} = \sum_{s=1}^S \mathbf{U}_{s,r_3}^{(3)} \mathbf{x}_{h,w,s}, \quad (4)$$

$$\mathbf{Z}'_{h',w',r_4} = \sum_{i=1}^D \sum_{j=1}^D \sum_{r_3=1}^{R_3} \mathbf{G}_{i,j,r_3,r_4} \mathbf{Z}_{h,w,r_3}, \quad (5)$$

$$\mathbf{Y}_{h',w',t} = \sum_{r_4=1}^{R_4} \mathbf{U}_{t,r_4}^{(4)} \mathbf{Z}'_{h',w',r_4}, \quad (6)$$

where  $\mathbf{Z}$  and  $\mathbf{Z}'$  are the intermediate output tensors. The above process is equivalent to a three-layer convolutional network without linear transformations, where the first convolutional layer from  $S$  feature maps to  $R_3$  feature maps with  $1 \times 1$  kernel size, the second convolutional layer from  $R_3$  feature maps to  $R_4$  feature maps with  $D \times D$  kernel size, the last convolutional layer from  $R_4$  feature maps to  $T$  feature maps with  $1 \times 1$  kernel size. This substructure is more common in other classical network structure, such as the inception module in GoogleNets, where there are no nonlinear layers between the  $1 \times 1$  and  $D \times D$  convolutional layers. The convolutional mapping process of TK-2 is shown in Figure 1.

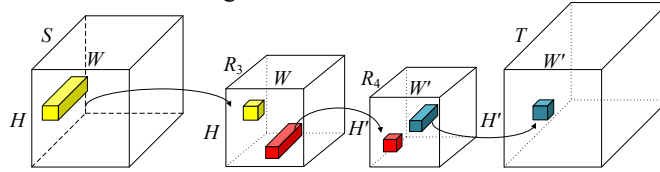


Fig. 1. TK-2 decompositions for compact a convolution.

### B. Low-rank TSVD representation of Fully Connected layers

For classical neural networks, the convolutional layer is a fourth-order tensor and the Fully Connected (FC) layer is a second-order matrix. The FC layer is computed as follows:

$$\mathbf{y}^T = \mathbf{x}^T \mathbf{W}, \quad (7)$$

where  $\mathbf{x} \in \mathbb{R}^M$  is an input vector,  $\mathbf{y} \in \mathbb{R}^N$  is an output vector, and  $\mathbf{W} \in \mathbb{R}^{M \times N}$  is a weight matrix. Since the weights are in matrix form and their order is not high, we use TSVD to compress the FC layer instead of CP or TK-2 decomposition. TSVD can decompose the weight matrix into three parts, which are the left singular matrix  $\mathbf{U} \in \mathbb{R}^{M \times R}$ , the right singular matrix  $\mathbf{V}^T \in \mathbb{R}^{R \times N}$ , and the diagonal singular value matrix  $\mathbf{S} \in \mathbb{R}^{R \times R}$ .  $R$  represents weight matrix rank. The larger the  $R$  the larger the compression ratio, but the more the model will lose performance. The decomposition process is as follows:

$$\mathbf{W} = \mathbf{U} \mathbf{S} \mathbf{V}^T, \quad (8)$$

Integrate the computational processes of the FC layer and TSVD with each other. It is easy to obtain the following form:

$$\mathbf{y}^T = (\mathbf{x}^T (\mathbf{US}))\mathbf{V}^T, \quad (9)$$

This means that a layer of full connectivity can be replaced by two consecutive sublayers. It can be expressed as follows:

$$\mathbf{z}^T = \mathbf{x}^T (\mathbf{US}), \quad (10)$$

$$\mathbf{y}^T = \mathbf{z}^T \mathbf{V}^T. \quad (11)$$

### C. Theoretical complexity analysis

The original convolution operation and FC layer require model parameters for  $D^2ST$  and  $MN$  and bring about computational consumption with  $H'W'D^2ST$  and  $MN$ . After compression, the theoretical compression ratio ( $CR$ ) and speed-up ratio ( $SR$ ) of the convolutional layer can be obtained by

$$CR = \frac{TSD^2}{RS + RD^2 + TR}, \quad (12)$$

$$SR = \frac{TSD^2W'H'}{RSWH + RD^2W'H' + TRW'H'}, \quad (13)$$

For an FC layer, the computation process is similar to that of a convolutional layer. We can consider an FC layer as a  $1 \times 1$  convolutional layer.

$$CR = SR = \frac{MN}{MR + RN}. \quad (14)$$

---

#### Algorithm 1: Orthogonal regularization training

---

**Input:** Dataset  $D$ , ranks  $\{R\}$ , TK-2 decomposition for each layer

$\mathbf{G} \in \mathbb{R}^{R1 \times R2 \times R3 \times R4}$   $\mathbf{U}^{(3)} \in \mathbb{R}^{S \times R3}$  and  $\mathbf{U}^{(4)} \in \mathbb{R}^{T \times R4}$ .

orthogonal parameters  $\rho, \lambda$ , training epochs  $E, e$ .

**Output:**  $\mathbf{U}^{(3)}, \mathbf{U}^{(4)}, \mathbf{G}$ .

**Initialize:** xavier\_uniform( $\mathbf{U}^{(3)}, \mathbf{U}^{(4)}, \mathbf{G}$ ).

// over-parameterized training

**for**  $t=1$  to  $E$  **do**

$\mathbf{X}, \mathbf{Y} \leftarrow$  sample\_batch( $D$ );

$\hat{\mathbf{Y}} \leftarrow$  forward( $\mathbf{X}, \{\mathbf{U}^{(3)}, \mathbf{U}^{(4)}, \mathbf{G}\}$ ) via (4), (5) and (6);

    // Orthogonal regularization

    Calculate  $L_{R3}$  via (15);

    Calculate  $L_{R4}$  via (16);

    Calculate  $L$  via (17);

    Udata ( $\{\mathbf{U}^{(3)}, \mathbf{U}^{(4)}, \mathbf{G}\},$  loss);

**end**

// low-rank training

**for**  $t$  to  $e$  **do**

    retraining ( $\{\mathbf{U}^{(3)}, \mathbf{U}^{(4)}, \mathbf{G}\},$  loss);

**end**

---

### D. Orthogonal regularization for CNNs

The factorized factor matrices satisfy orthogonality for both TK-2 and SVD, which provide sufficient theories guarantee for low-rank approximation. However, the factor matrix acts as a free variable in the decomposition process and it will be updated at each iteration. Therefore, its orthogonality is difficult to be guaranteed. It is essential to employ various optimization strategies [71]-[80].

To improve the performance of the compression model while reducing the computational and storage expenses, we adopt a high-rank regularization training strategy [81]-[85]. Specifically, the weight tensor is first decomposed with high rank, and the model is more honorably close to the accuracy of the original model due to its large number of parameters. Second, orthogonal regularization is applied to the factor matrix of the decomposition [86]-[90]. The rationale for training based on this idea is that orthogonality maximizes the ability to represent information. The orthogonal regularization is calculated as follows:

$$L_{R_3}(U^{(3)}) = \frac{\rho}{R_3} (\|U^{(3)T}U^{(3)} - I\|_F^2 + \|U^{(3)}U^{(3)T} - I\|_F^2), \quad (15)$$

$$L_{R_4}(U^{(4)}) = \frac{\rho}{R_4} (\|U^{(4)T}U^{(4)} - I\|_F^2 + \|U^{(4)}U^{(4)T} - I\|_F^2), \quad (16)$$

where  $\rho$  denotes regularization strength,  $\|\cdot\|_F$  is the Frobenius norm. Orthogonality of the factor matrix  $U^{(3)}$  is expressed by minimizing the residual matrix  $L_{R_3}$ . If  $U^{(3)}$  exhibits strong orthogonality, then  $L_{R_3}$  will be small. Therefore, the following loss can be modeled for the model.

$$L = L_{ce} + \lambda(L_{R_3}(U^{(3)}) + L_{R_4}(U^{(4)})), \quad (17)$$

where  $L_{ce}$  is loss function, e.g. cross-entropy loss in classification tasks, and the second term is regularization loss.  $\lambda$  is a weight parameter. The whole training process is shown in Algorithm 1.

### E. Rank Selection

In tensor decomposition, the choice of rank is crucial for model compression because it directly affects the accuracy and efficiency of the compressed model. The rank is the dimension of the core tensor in the decomposed tensor, and a lower rank means fewer parameters, which can reduce the storage requirements and computational complexity of the model. However, too low a rank may lead to information loss and affect the prediction accuracy of the model.

In this paper, VBMF (Variational Bayesian Matrix Factorization) is used to estimate the matrix or tensor rank. VBMF is based on Bayesian inference, which estimates the rank of a matrix or tensor by introducing a prior distribution and is particularly suitable for high-dimensional data. The basic idea of VBMF is to decompose the matrix or tensor into a low-rank part and a noise part and then use Bayesian inference to estimate the parameters of these parts, including the rank of the low-rank part. The VBMF method automatically adjusts the complexity of the model and takes into account the noise in the data. In VBMF, for a given matrix or tensor, variational inference can be used to estimate the parameters of its low-rank and noise parts. In this case, the estimation of the rank is done by maximizing the posterior probability. By iteratively updating the parameters, the rank value that maximizes the a posteriori probability can be found.

VBMF can efficiently estimate the tensor rank. However, for CNNs, there is a significant imbalance in the weight tensor, i.e., the input and output channels may not be equal. Decomposing different modalities using the same set of tensor ranks usually results in a severe loss of accuracy. Meanwhile, the potential relationship between the input and output channels, such as the multiplicative relationship, is taken into account. Therefore, the VBMF is only used to determine the rank of the third modal matrix. The rank of the fourth modal matrix can be obtained simply from the relationship between the channels.

TABLE I STATISTICAL INFORMATION ON CIFAR10 AND SVHN

Datasets	class	Train	Test	Size
D1	10	$5 \times 10^4$	$1 \times 10^4$	$32 \times 32$
D2	100	$5 \times 10^4$	$1 \times 10^4$	$32 \times 32$

## IV. EXPERIMENTS

We tested the effectiveness of the method by testing ResNet18 and ResNet20 on the CIFAR-10 and CIFAR-100 datasets, respectively.

### A. Data preparation

Different datasets will be used to evaluate the performance of the compression model. The informative statistics of the different datasets are displayed in Table I.

**D1(CIFAR-10):** It is a widely used standard dataset for computer vision for training and evaluating machine learning models, especially in the field of image recognition.

**D2(CIFAR-100):** It is a real image dataset widely used in the development of machine learning and image classification algorithms. The CIFAR-100 dataset is commonly used in deep learning research, especially in the field of CNNs and unsupervised feature learning.

### B. Evaluation Metrics

**Top-1 accuracy (Top-1):** It is the proportion of the model's predictions for the most likely category (i.e., the prediction with the highest probability) that agrees with the true label. In other words, a prediction is considered correct if the model predicts exactly the right category as its first choice. Specific definitions are given below:

$$\text{Top-1} = \frac{f}{F} \times 100\%, \quad (18)$$

where  $F$  denotes the total number of test samples.  $f$  denotes the number of correctly predicted samples, i.e., the number of samples for which the model’s Top-1 prediction matches the actual label.

**Compression ratio:** The compression ratio of a neural network is the ratio of the compressed model parameters to the original model parameters. It is defined as follows:

$$\text{CR} = \frac{P_{\text{original}}}{P_{\text{compressed}}}, \quad (19)$$

Where  $P_{\text{compressed}}$  and  $P_{\text{original}}$  denote the parameters after compression and before compression, respectively.

### C. Experimental platforms and setups.

The experiments are conducted using PyTorch within the Tensorly toolbox. These experiments run on a desktop computer equipped with 2.50 GHz Intel Cores and 12 GB of RAM. The batch size is set to 128, and the initial learning rate is configured at 0.1. This rate is then decreased to 0.01 after the 100th epoch and further reduce to 0.001 after the 150th epoch.

### D. Experimental results analysis

Through extensive experiments, we obtained the results shown in Tables II, III, IV, and V.

**ResNet20 on CIFAR-10.** Table II compares our method TK-2 format ResNet-20 models with the state-of-the-art model compression method on the CIFAR-10 dataset. Some sparse compression methods, such as GrowEfficient and BackSparse, introduce a serious performance degradation to the model, even though the compression is relatively small. SVDT performs similarly on the CIFAR-10 dataset. In contrast, the PSTRN-S method obtains 0.19% accuracy improvement with a similar compression ratio 2.70×. It is exciting that our approach achieves state-of-the-art results, both in terms of accuracy and compression rate. Especially when the compression ratio is small, our method can obtain an accuracy improvement of 0.22% with a moderate compression ratio 2.00× compared to the original model.

**ResNet20 on CIFAR-100.** Table III shows the experimental results on CIFAR-100. Our compression model outperforms other work when the compression ratio is small. With 2.30× compression ratio, our model achieves 66.96% Top-1 accuracy, which is even 1.56% higher than the uncompressed model. If the compression ratio exceeds 4, the accuracy of the model suffers a severe degradation, both for the state-of-the-art BATUDE and the method proposed in this paper. Even so, the method in this paper maintains sufficient toughness in terms of comprehensive performance.

**ResNet32 on CIFAR-10.** Table VI shows the experimental results on CIFAR-10. ResNet32 has a deeper residual structure compared to ResNet20, so the classification accuracy obtained will be higher. Similar to the previous results, utilizing sparsity for model compression brings a non-negligible accuracy loss, even if the compression is relatively small. For some advanced low-rank models such as PSTRN-S, it has 1.05% accuracy drop with compression ratio 2.60×. However, our model even outperforms the uncompressed model with 0.5% accuracy increase.

**ResNet32 on CIFAR-100.** Table V shows the experimental results on CIFAR-100. Again, our approach still achieves state-of-the-art performance. The loss of accuracy is more pronounced in both PSTRN-M and PSTRN-S. In contrast, BATUDE, a low-rank decomposition model, exhibits strong compression. Similar results are achieved with our method when the compression is relatively large. However, when the compression ratio is small, our method is more advantageous. Specifically, our method can obtain an accuracy improvement of 0.26% with a moderate compression ratio 2.00× compared to the original model.

TABLE II RESNET20 ON CIFAR-10 DATASET

Method	Post-Train Model	Top-1 (%)	CR
Original			
ResNet-20	Dense	91.25	1.00×
SVDT [91]	Low-rank	90.39	2.94×
PSTRN-S [92]	Low-rank	91.44	2.70×
GE [93]	Sparse	90.91	2.00×
BS [94]	Sparse	90.73	2.77×
<b>Ours</b>	Low-rank	91.79	2.00×
<b>Ours</b>	Low-rank	89.42	4.26×

TABLE III RESNET20 ON CIFAR-100 DATASET

Method	Post-Train Model	Top-1 (%)	CR
--------	------------------	-----------	----

Original ResNet-20	Dense	65.40	1.00×
PSTRN-M [92]	Low-rank	63.62	4.70×
PSTRN-S [92]	Low-rank	66.13	2.30×
BATUDE [34]	Low-rank	64.91	4.70×
BATUDE [34]	Low-rank	66.67	2.80×
<b>Ours</b>	Low-rank	66.96	2.00×
<b>Ours</b>	Low-rank	65.12	4.26×

TABLE VI RESNET32 ON CIFAR-10 DATASET

Method	Post-Train Model	Top-1 (%)	CR
Original ResNet-32	Dense	92.49	1.00×
FPGM [95]	Sparse	91.93	2.12×
SCOP [96]	Sparse	92.13	2.27×
SVDt [91]	Low-rank	90.55	3.93×
PSTRN-S [92]	Low-rank	91.44	2.60×
<b>Ours</b>	Low-rank	92.99	2.00×
<b>Ours</b>	Low-rank	91.07	4.26×

TABLE V RESNET32 ON CIFAR-100 DATASET

Method	Post-Train Model	Top-1 (%)	CR
Original ResNet-32	Dense	68.10	1.00×
PSTRN-M [92]	Low-rank	59.03	2.50×
PSTRN-S [92]	Low-rank	66.77	5.20×
BATUDE [34]	Low-rank	68.05	2.40×
BATUDE [34]	Low-rank	66.96	5.20×
<b>Ours</b>	Low-rank	68.37	2.00×
<b>Ours</b>	Low-rank	67.01	4.26×

## V. CONCLUSIONS

In this paper, we propose a model compression framework Based on low-rank representation learning that incorporates orthogonal regularization and VBMF. In this framework, over-parameterization and orthogonal regularization training provide orthogonal properties for low-rank models. In addition, the VBMF estimates the rank of one modality of the weight tensor, and the other rank is solved taking into account the imbalance between channels. It avoids that one modality of the tensor affects the model performance because it is over-compressed. Experiments show that the method in this paper outperforms the state-of-the-art models in terms of compression rate and test accuracy.

In the future, we will design novel tensor decomposition methods to achieve a balance between model parameters and accuracy. Meanwhile, to increase the compression rate of the model, we will synergistically explore different compression methods, such as low-rank decomposition combined with pruning and quantization.

## REFERENCES

- [1] N. Zeng, X. Li, P. Wu, H. Li and X. Luo, "A Novel Tensor Decomposition-Based Efficient Detector for Low-Altitude Aerial Objects With Knowledge Distillation Scheme," *IEEE/CAA J. Autom. Sinica*, vol. 11, no. 2, pp. 487-501, Feb. 2024.
- [2] L. Wei, L. Jin and X. Luo, "Noise-Suppressing Neural Dynamics for Time-Dependent Constrained Nonlinear Optimization With Applications," *IEEE Trans. Syst. Man Cybern. Syst.*, vol. 52, no. 10, pp. 6139-6150, Oct. 2022.
- [3] L. Jin, Y. Qi, X. Luo, S. Li, and M. Shang, "Distributed Competition of Multi-Robot Coordination Under Variable and Switching Topologies," *IEEE Trans. Autom. Sci. Eng.*, vol. 19, no. 4, pp. 3575-3586, Oct. 2022.
- [4] D. Feng, A. Harakeh, S. L. Waslander, and K. Dietmayer, "A Review and Comparative Study on Probabilistic Object Detection in Autonomous Driving," *IEEE Trans. Intell. Transp. Syst.*, vol. 23, no. 8, pp. 9961-9980, Aug. 2022.
- [5] Z. Liu, X. Luo and Z. Wang, "Convergence Analysis of Single Latent Factor-Dependent, Nonnegative, and Multiplicative Update-Based Nonnegative Latent Factor Models," *IEEE Trans. Neural Netw. Learn. Syst.*, vol. 32, no. 4, pp. 1737-1749, Apr. 2021.
- [6] X. Luo, H. Wu, and Z. Li, "NeuLFT: A novel approach to nonlinear canonical polyadic decomposition on high-dimensional incomplete tensors," *IEEE Trans. Knowl. Data Eng.*, vol. 35, no. 6, pp. 6148-6166, Jun. 2023.
- [7] X. Luo, D. Wang, M. Zhou, and H. Yuan, "Latent Factor-Based Recommenders Relying on Extended Stochastic Gradient Descent Algorithms," *IEEE Trans. Syst. Man Cybern. Syst.*, vol. 51, no. 2, pp. 916-926, Feb. 2021.
- [8] Y. He, Y. Su, X. Wang, J. Yu, and Y. Luo, "An improved method MSS-YOLOv5 for object detection with balancing speed-accuracy", *Front. Phys.*, vol. 10, pp. 1101923, 2023.
- [9] S. Deng, Q. Hu, D. Wu, and Y. He, "BCTC-KSM: A blockchain-assisted threshold cryptography for key security management in power IoT data sharing," *Comput. Electr. Eng.*, vol. 108, pp: 108666, 2023.
- [10] X. Luo, W. Qin, A. Dong, K. Sedraoui and M. Zhou, "Efficient and High-quality Recommendations via Momentum-incorporated Parallel Stochastic Gradient Descent-Based Learning," *IEEE/CAA J. Autom. Sin.*, vol. 8, no. 2, pp. 402-411, Feb. 2021.
- [11] M. Masana, X. Liu, B. Twardowski, M. Menta, A. D. Bagdanov, and J. van de Weijer, "Class-Incremental Learning: Survey and Performance Evaluation on Image Classification," *IEEE Trans. Pattern Anal. Mach. Intell.*, vol. 45, no. 5, pp. 5513-5533, May 2023.
- [12] G. Cheng, X. Yuan, X. Yao, K. Yan, Q. Zeng, X. Xie, and J. Han, "Towards Large-Scale Small Object Detection: Survey and Benchmarks," *IEEE Trans. Pattern Anal. Mach. Intell.*, vol. 45, no. 11, pp. 13467-13488, Nov. 2023.
- [13] M. Chen, R. Wang, Y. Qiao, and X. Luo, "A Generalized Nesterov's Accelerated Gradient-Incorporated Non-Negative Latent-Factorization-of-Tensors Model for Efficient Representation to Dynamic QoS Data," *IEEE Trans. Emerg. Top. Comput. Intell.*, vol. 8, no. 3, pp. 2386-2400, Jun. 2024.
- [14] Q. Wang and H. Wu, "Dynamically Weighted Directed Network Link Prediction Using Tensor Ring Decomposition," *27th Int. Conf. Comput. Supported Cooperative Work Des.*, 2024, Tianjin, China, pp. 2864-2869.
- [15] X. Luo, M. Chen, H. Wu, Z. Liu, H. Yuan, and M. Zhou, "Adjusting Learning Depth in Nonnegative Latent Factorization of Tensors for Accurately Modeling Temporal Patterns in Dynamic QoS Data," *IEEE Trans. Autom. Sci. Eng.*, vol. 18, no. 4, pp. 2142-2155, Oct. 2021.
- [16] S. Y. Chang and H. -C. Wu, "Tensor Quantization: High-Dimensional Data Compression," *IEEE Trans. Circuits Syst. Video Technol.*, vol. 32, no. 8, pp. 5566-5580, Aug. 2022.
- [17] H. Wu, X. Luo, M. Zhou, M. J. Rawa, K. Sedraoui, and A. Albeshri, "A PID-incorporated Latent Factorization of Tensors Approach to Dynamically Weighted Directed Network Analysis," *IEEE/CAA J. Autom. Sin.*, vol. 9, no. 3, pp. 533-546, Mar. 2022.
- [18] W. Qin, H. Wang, F. Zhang, J. Wang, X. Luo and T. Huang, "Low-Rank High-Order Tensor Completion With Applications in Visual Data," *IEEE Trans. Image Process.*, vol. 31, pp. 2433-2448, Mar. 2022.
- [19] H. Wu, X. Wu, and X. Luo, "Dynamic Network Representation Based on Latent Factorization of Tensors," Springer, Mar. 2023.
- [20] W. Li, X. Luo, H. Yuan, and M. Zhou, "A Momentum-Accelerated Hessian-Vector-Based Latent Factor Analysis Model," *IEEE Trans. Serv. Comput.*, vol. 16, no. 2, pp. 830-844, 1 Mar.-Apr. 2023.
- [21] X. Wang, L. T. Yang, Y. Wang, L. Ren, and M. J. Deen, "ADTT: A Highly Efficient Distributed Tensor-Train Decomposition Method for IIoT Big Data," *IEEE Trans. Ind. Informat.*, vol. 17, no. 3, pp. 1573-1582, Mar. 2021.
- [22] M.Chen, C. He, and X. Luo, "MNL: A Highly-Efficient model for Large-scale Dynamic Weighted Directed Network Representation," *IEEE Trans. on Big Data*, vol. 9, no. 3, pp. 889-903, Oct. 2023.
- [23] X. Luo, H. Wu, Z. Wang, J. Wang, and D. Meng, "A Novel Approach to Large-Scale Dynamically Weighted Directed Network Representation," *IEEE Trans. Pattern Anal. Mach. Intell.*, vol. 44, no. 12, pp. 9756-9773, 1 Dec. 2022.
- [24] J. Chen, X. Luo and M. Zhou, "Hierarchical Particle Swarm Optimization-incorporated Latent Factor Analysis for Large-Scale Incomplete Matrices," *IEEE Trans. Big Data*, vol. 8, no. 6, pp. 1524-1536, 1 Dec. 2022.
- [25] L. Hu, S. Yang, X. Luo, H. Yuan, K. Sedraoui, and M. Zhou, "A Distributed Framework for Large-scale Protein-protein Interaction Data Analysis and Prediction Using MapReduce," *IEEE/CAA J. Autom. Sin.*, vol. 9, no. 1, pp. 160-172, Jan. 2022.
- [26] Z. Wang, Y. Liu, X. Luo, J. Wang, C. Gao, D. Peng, and W.Chen, "Large-Scale Affine Matrix Rank Minimization With a Novel Nonconvex Regularizer," *IEEE Trans. Neural Networks Learn. Syst.*, vol. 33, no. 9, pp. 4661-4675, Sept. 2022.
- [27] Y. Wang, H. Wu, J. Zhang, Z. Gao, J. Wang, P. Yu, and M. Long, "PredRNN: A Recurrent Neural Network for Spatiotemporal Predictive Learning," *IEEE Trans. Pattern Anal. Mach. Intell.*, vol. 45, no. 2, pp. 2208-2225, Feb. 2023.
- [28] J. Feng, L. T. Yang, B. Ren, D. Zou, M. Dong, and S. Zhang, "Tensor Recurrent Neural Network With Differential Privacy," *IEEE Trans. Comput.*, vol. 73, no. 3, pp. 683-693, Mar. 2024.
- [29] L. T. Thanh, K. Abed-Meraim, N. L. Trung, and A. Hafiane, "A Contemporary and Comprehensive Survey on Streaming Tensor Decomposition," *IEEE Trans. Knowl. Data Eng.*, vol. 35, no. 11, pp. 10897-10921, 1 Nov. 2023.
- [30] D. Wang, B. Wu, G. Zhao, M. Yao, H. Chen, L. Deng, T. Yan, and G. Li, "Kronecker CP Decomposition With Fast Multiplication for Compressing RNNs," *IEEE Trans. Neural Networks Learn. Syst.*, vol. 34, no. 5, pp. 2205-2219, May 2023.
- [31] Y. Pan, J. Xu, M. Wang, J. Ye, F. Wang, K. Bai, and Z. Xu, "Compressing Recurrent Neural Networks with Tensor Ring for Action Recognition," *33rd Proc. AAAI Conf. Artif. Intell.*, 2019, Hawaii, USA, vol.33, no. 1, pp: 4683-4690.
- [32] R. Balestriero, L. Bottou, Y. LeCun, "The Effects of Regularization and Data Augmentation are Class Dependent," *35th Adv. Neural Inf. Process. Syst.*, 2022, New Orleans, United States, pp: 37878-37891.



- [33] J.Zhang, F. Zhan, M. Xu, S. Lu, and E. Xing, "FreGS: 3D Gaussian Splatting with Progressive Frequency Regularization," in *40th Proc. IEEE/CVF Conf. Comput. Vis. Pattern Recognit.*, 2024, Seattle, United States, pp. 21424-21433.
- [34] M. Yin, H. Phan, X. Zang, S. Liao, and B. Yuan, "BATUDE: Budget-Aware Neural Network Compression Based on Tucker Decomposition," in *Proc. 36th AAAI Conf. Artif. Intell.*, Online, 2022, vol.36, no. 8, pp: 8874-8882.
- [35] D. Wu, X. Luo, Y. He, and M. Zhou, "A Prediction-Sampling-Based Multilayer-Structured Latent Factor Model for Accurate Representation to High-Dimensional and Sparse Data," *IEEE Trans. Neural Networks Learn. Syst.*, vol. 35, no. 3, pp. 3845-3858, Mar. 2024.
- [36] X. Luo, Y. Zhou, Z. Liu, and M. Zhou, "Fast and Accurate Non-Negative Latent Factor Analysis of High-Dimensional and Sparse Matrices in Recommender Systems," *IEEE Trans. Knowl. Data Eng.*, vol. 35, no. 4, pp. 3897-3911, Apr. 2023.
- [37] X. Zhou, W. Zhong, Z. Chen, S. Diao, and T. Zhang, "Efficient Neural Network Training via Forward and Backward Propagation Sparsification," *Adv. Neural Inf. Process. Syst.*, vol. 34, pp: 15216-15229, 2021.
- [38] D. Wu, Y. He and X. Luo, "A Graph-Incorporated Latent Factor Analysis Model for High-Dimensional and Sparse Data," *IEEE Trans. Emerg. Top. Comput.*, vol. 11, no. 4, pp. 907-917, Oct.-Dec. 2023.
- [39] Y. Yuan, X. Luo, M. Shang, and Z. Wang, "A Kalman-Filter-Incorporated Latent Factor Analysis Model for Temporally Dynamic Sparse Data," *IEEE Trans. Syst. Man Cybern. Syst.*, vol. 53, no. 9, pp. 5788-5801, Sept. 2023.
- [40] Y. He, P. Liu, Z. Wang, Z. Hu, and Y. Yang. "Filter pruning via geometric median for deep convolutional neural networks acceleration," in *Proc. 32nd IEEE/CVF Conf. Comput. Vis. Pattern Recognit.*, 2019, Long Beach, pp: 4340-4349.
- [41] Y. Yuan, Q. He, X. Luo and M. Shang, "A Multilayered-and-Randomized Latent Factor Model for High-Dimensional and Sparse Matrices," *IEEE Trans. Big Data*, vol. 8, no. 3, pp. 784-794, 1 June 2022.
- [42] D. Wu, Y. He, X. Luo and M. Zhou, "A Latent Factor Analysis-Based Approach to Online Sparse Streaming Feature Selection," *IEEE Trans. Syst. Man Cybern. Syst.*, vol. 52, no. 11, pp. 6744-6758, Nov. 2022.
- [43] Y. He and L. Xiao, "Structured Pruning for Deep Convolutional Neural Networks: A Survey," *IEEE Trans. Pattern Anal. Mach. Intell.*, vol. 46, no. 5, pp. 2900-2919, May 2024.
- [44] P. Wimmer, J. Mehnert, and A. Condurache, "Interspace Pruning: Using Adaptive Filter Representations To Improve Training of Sparse CNNs," in *Proc. 39th IEEE/CVF Conf. Comput. Vis. Pattern Recognit.*, 2022, New Orleans, USA, pp. 12527-12537.
- [45] W. Qin, X. Luo and M. Zhou, "Adaptively-Accelerated Parallel Stochastic Gradient Descent for High-Dimensional and Incomplete Data Representation Learning," *IEEE Trans. Big Data*, vol. 10, no. 1, pp. 92-107, Feb. 2024.
- [46] W. Qin and X. Luo, "Asynchronous Parallel Fuzzy Stochastic Gradient Descent for High-Dimensional Incomplete Data Representation," *IEEE Trans. Fuzzy Syst.*, vol. 32, no. 2, pp. 445-459, Feb. 2024.
- [47] J. Q. Xiao, C. M. Zhang, Y. Gong, M. Yin, Y Sui, L. Z. Xiang, D. W. Tao, and B. Yuan, "HALOC: Hardware-aware Automatic Low-Rank Compression for Compact Neural Networks," in *Proc. 37th AAAI Conf. Artif. Intell.*, Washington D.C., USA, 2023, pp. 10464-10472.
- [48] B. Chen, J. Guan, and Z. Li, "Unsupervised Feature Selection via Graph Regularized Nonnegative CP Decomposition," *IEEE Trans. Pattern Anal. Mach. Intell.*, vol. 45, no. 2, pp. 2582-2594, 2023.
- [49] X. Tuo, Y. Zhang, Y. Huang, and J. Yang, "Fast Sparse-TSVD Super-Resolution Method of Real Aperture Radar Forward-Looking Imaging," *IEEE Trans. Geosci. Remote Sens.*, vol. 59, no. 8, pp. 6609-6620, Aug. 2021.
- [50] M. Yin, Y. Sui, W. Yang, X. Zang, Y. Gong, and B. Yuan, "HODEC: Towards Efficient High-order Decomposed Convolutional Neural Networks," in *Proc. 35th IEEE/CVF Conf. Comput. Vis. Pattern Recognit.*, New Orleans, USA, 2022, pp. 12299-12308.
- [51] L. Jin, X. Zheng and X. Luo, "Neural Dynamics for Distributed Collaborative Control of Manipulators With Time Delays," *IEEE/CAA J. Autom. Sin.*, vol. 9, no. 5, pp. 854-863, May 2022.
- [52] W. Yang, S. Li, Z. Li and X. Luo, "Highly Accurate Manipulator Calibration via Extended Kalman Filter-Incorporated Residual Neural Network," *IEEE Trans. Ind. Informat.*, vol. 19, no. 11, pp. 10831-10841, Nov. 2023.
- [53] L. Chen and X. Luo, "Tensor Distribution Regression Based on the 3D Conventional Neural Networks," *IEEE/CAA J. Autom. Sin.*, vol. 10, no. 7, pp. 1628-1630, Jul. 2023.
- [54] L. Wei, L. Jin and X. Luo, "Noise-Suppressing Neural Dynamics for Time-Dependent Constrained Nonlinear Optimization With Applications," *IEEE Trans. Syst. Man Cybern. Syst.*, vol. 52, no. 10, pp. 6139-6150, Oct. 2022.
- [55] Y. Zheng, T. Huang, X. Zhao, Q. Zhao, and T. Jiang, "Fully-Connected Tensor Network Decomposition and Its Application to Higher-Order Tensor Completion," *35th Proc. AAAI Conf. Artif. Intell.*, 2021, Online, vol.35, no. 12, pp: 4683-4690.
- [56] V. Aggarwal, W. Wang, B. Eriksson, Y. Sun, and W. Wang, "Wide Compression: Tensor Ring Nets," in *Proc. 31st IEEE/CVF Conf. Comput. Vis. Pattern Recognit.*, Hawaii, USA, 2018, pp. 9329-9338.
- [57] H. Wu and X. Luo, "Instance-Frequency-Weighted Regularized, Nonnegative and Adaptive Latent Factorization of Tensors for Dynamic QoS Analysis," *IEEE Int. Conf. Web Serv.*, 2021, Chicago, USA, 2021, pp. 560-568.
- [58] H. Wu, X. Luo and M. Zhou, "Neural Latent Factorization of Tensors for Dynamically Weighted Directed Networks Analysis," *IEEE Int. Conf. Syst. Man Cybern.*, 2021, Melbourne, Australia, pp. 3061-3066.
- [59] D. Wu, P. Zhang, Y. He, and X. Luo, "A Double-Space and Double-Norm Ensembled Latent Factor Model for Highly Accurate Web Service QoS Prediction," *IEEE Trans. Serv. Comput.*, vol. 16, no. 2, pp. 802-814, 1 Mar.-Apr. 2023.
- [60] Z. Xie, L. Jin and X. Luo, "Kinematics-Based Motion-Force Control for Redundant Manipulators With Quaternion Control," *IEEE Trans. Autom. Sci. Eng.*, vol. 20, no. 3, pp. 1815-1828, Jul. 2023.
- [61] W. Li, R. Wang, X. Luo and M. Zhou, "A Second-Order Symmetric Non-Negative Latent Factor Model for Undirected Weighted Network Representation," *IEEE Trans. Netw. Sci. Eng.*, vol. 10, no. 2, pp. 606-618, 1 Mar.-Apr. 2023.
- [62] Y. Yuan, R. Wang, G. Yuan and L. Xin, "An Adaptive Divergence-Based Non-Negative Latent Factor Model," *IEEE Trans. Syst. Man Cybern. Syst.*, vol. 53, no. 10, pp. 6475-6487, Oct. 2023.
- [63] C. Li, C.shi, "Constrained Optimization Based Low-Rank Approximation of Deep Neural Networks," in *31st Proc. Eur. Conf. Comput. Vis.*, 2018, Salt Lake City, USA, pp:732-747.
- [64] M. Li, Y. Liu, B. Wong, V. Gan, J. Cheng, "Automated structural design optimization of steel reinforcement using graph neural network and exploratory genetic algorithms." *Autom. Constr.* vol. 146 pp: 1-16, Feb. 2023.

- [65] W. Deng, X. Zhang, Y. Zhou, Y. Liu, X. Zhou, H. Chen, and H. Zhao, "An enhanced fast non-dominated solution sorting genetic algorithm for multi-objective problems," *Inf. Sci.*, vol. 585, pp. 1-13, Mar. 2021.
- [66] M. Beniwal, A. Singh, N. Kumar, "Forecasting long-term stock prices of global indices: A forward-validating Genetic Algorithm optimization approach for Support Vector Regression," *Appl. Soft Comput.*, vol. 145, pp. 1-15, Mar. 2023.
- [67] T. Chen, S. Li, Y. Qiao, and X. Luo, "A Robust and Efficient Ensemble of Diversified Evolutionary Computing Algorithms for Accurate Robot Calibration," *IEEE Trans. Instrum. Meas.*, vol. 73, pp. 1-14, Feb. 2024.
- [68] H. Wu, X. Luo and M. Zhou, "Discovering Hidden Pattern in Large-scale Dynamically Weighted Directed Network via Latent Factorization of Tensors," *IEEE 17th Int. Conf. Autom. Sci. Eng.*, 2021, Lyon, France, pp. 1533-1538.
- [69] H. Wu, Y. Xia and X. Luo, "Proportional-Integral-Derivative-Incorporated Latent Factorization of Tensors for Large-Scale Dynamic Network Analysis," *China Autom. Congr.*, 2021, Beijing, China, pp. 2980-2984.
- [70] L. Acerbi, "Variational Bayesian Monte Carlo with Noisy Likelihoods," *33rd Adv. Neural Inf. Process. Syst.*, 2020, Online, pp: 8211-8222.
- [71] F. Bi, X. Luo, B. Shen, H. Dong, and Z. Wang, "Proximal Alternating-Direction-Method-of-Multipliers-Incorporated Nonnegative Latent Factor Analysis," *IEEE/CAA J. Autom. Sin.*, vol. 10, no. 6, pp. 1388-1406, Jun. 2023.
- [72] Y. Zhong, K. Liu, S. Gao, and X. Luo, "Alternating-Direction-Method of Multipliers-Based Adaptive Nonnegative Latent Factor Analysis," *IEEE Trans. Emerg. Top. Comput. Intell.*, doi: 10.1109/TETCI.2024.3420735.
- [73] X. Luo, Y. Zhong, Z. Wang, and M. Li, "An Alternating-Direction-Method of Multipliers-Incorporated Approach to Symmetric Non-Negative Latent Factor Analysis," *IEEE Trans. Neural Netw. Learn. Syst.*, vol. 34, no. 8, pp. 4826-4840, Aug. 2023.
- [74] W. Deng, J. Xu, X. -Z. Gao and H. Zhao, "An Enhanced MSIQDE Algorithm With Novel Multiple Strategies for Global Optimization Problems," *IEEE Trans. Syst. Man Cybern. Syst.*, vol. 52, no. 3, pp. 1578-1587, March 2022.
- [75] L. Hu, Y. Yang, Z. Tang, Y. He, and X. Luo, "FCAN-MOPSO: An Improved Fuzzy-Based Graph Clustering Algorithm for Complex Networks With Multiobjective Particle Swarm Optimization," *IEEE Trans. Fuzzy Syst.*, vol. 31, no. 10, pp. 3470-3484, Oct. 2023.
- [76] X. Luo, J. Chen, Y. Yuan, and Z. Wang, "Pseudo Gradient-Adjusted Particle Swarm Optimization for Accurate Adaptive Latent Factor Analysis," *IEEE Trans. Syst. Man Cybern. Syst.*, vol. 54, no. 4, pp. 2213-2226, Apr. 2024.
- [77] X. Sun, Z. Shi, G. Lei, Y. Guo, and J. Zhu, "Multi-Objective Design Optimization of an IPMSM Based on Multilevel Strategy," *IEEE Trans. Ind. Electron.*, vol. 68, no. 1, pp. 139-148, Jan. 2021.
- [78] C. He, R. Cheng, and D. Yazdani, "Adaptive Offspring Generation for Evolutionary Large-Scale Multiobjective Optimization," *IEEE Trans. Syst. Man Cybern. Syst.*, vol. 52, no. 2, pp. 786-798, Feb. 2022.
- [79] Z. Xie, L. Jin, X. Luo, M. Zhou, and Y. Zheng, "A Biobjective Scheme for Kinematic Control of Mobile Robotic Arms With Manipulability Optimization," *IEEE/ASME Trans. Mechatron.*, vol. 29, no. 2, pp. 1534-1545, Apr. 2024.
- [80] X. Luo, Y. Yuan, S. Chen, N. Zeng, and Z. Wang, "Position-Transitional Particle Swarm Optimization-Incorporated Latent Factor Analysis," *IEEE Trans. Knowl. Data Eng.*, vol. 34, no. 8, pp. 3958-3970, Aug. 2022.
- [81] X. Xu, M. Lin, X. Luo, and Z. Xu, "HRST-LR: A Hessian Regularization Spatio-Temporal Low Rank Algorithm for Traffic Data Imputation," *IEEE Trans. Intell. Transp. Syst.*, vol. 24, no. 10, pp. 11001-11017, Oct. 2023.
- [82] Y. Cui, W. Che, T. Liu, B. Qin, and Z. Yang, "Pre-Training With Whole Word Masking for Chinese BERT," *IEEE/ACM Trans. Audio, Speech, Language Process.*, vol. 29, pp. 3504-3514, 2021.
- [83] Z. Li, S. Li, O. O. Bamasag, A. Alhothali, and X. Luo, "Diversified Regularization Enhanced Training for Effective Manipulator Calibration," *IEEE Trans. Neural Netw. Learn. Syst.*, vol. 34, no. 11, pp. 8778-8790, Nov. 2023.
- [84] H. Wu, X. Luo and M. Zhou, "Advancing Non-Negative Latent Factorization of Tensors With Diversified Regularization Schemes," *IEEE Trans. Serv. Comput.*, vol. 15, no. 3, pp. 1334-1344, May 2022.
- [85] B. Li, W. Zhang, M. Tian, G. Zhai, and X. Wang, "Blindly Assess Quality of In-the-Wild Videos via Quality-Aware Pre-Training and Motion Perception," *IEEE Trans. Circuits Syst. Video Technol.*, vol. 32, no. 9, pp. 5944-5958, Sept. 2022.
- [86] Z. Liu, G. Yuan and X. Luo, "Symmetry and Nonnegativity-Constrained Matrix Factorization for Community Detection," *IEEE/CAA J. Autom. Sin.*, vol. 9, no. 9, pp. 1691-1693, Sept. 2022.
- [87] Q. Wang, X. Liu, T. Shang, Z. Liu, H. Yang, and X. Luo, "Multi-Constrained Embedding for Accurate Community Detection on Undirected Networks," *IEEE Trans. Netw. Sci. Eng.*, vol. 9, no. 5, pp. 3675-3690, 1 Sept.-Oct. 2022.
- [88] Z. Liu, Y. Yi and X. Luo, "A High-Order Proximity-Incorporated Nonnegative Matrix Factorization-Based Community Detector," *IEEE Trans. Emerg. Top. Comput. Intell.*, vol. 7, no. 3, pp. 700-714, Jun. 2023.
- [89] Z. Liu, X. Luo and M. Zhou, "Symmetry and Graph Bi-Regularized Non-Negative Matrix Factorization for Precise Community Detection," *IEEE Trans. Autom. Sci. Eng.*, vol. 21, no. 2, pp. 1406-1420, Apr. 2024.
- [90] X. Luo, Z. Liu, L. Jin, Y. Zhou, and M. Zhou, "Symmetric Nonnegative Matrix Factorization-Based Community Detection Models and Their Convergence Analysis," *IEEE Trans. Neural Netw. Learn. Syst.*, vol. 33, no. 3, pp. 1203-1215, Mar. 2022.
- [91] H. Yang, M. Tang, W. Wen, F. Yan, D. Hu, A. Li, and Y. Chen, "Learning low-rank deep neural networks via singular vector orthogonality regularization and singular value sparsification," in *Proc. 34th IEEE/CVF Conf. Comput. Vis. Pattern Recognit. Workshops*, 2020, Online, pp. 678-679.
- [92] N. Li, Y. Pan, Y. Chen, Z. Ding, D. Zhao, and Z. Xu, "Heuristic rank selection with progressively searching tensor ring network," *Complex Intell. Syst.*, vol. 17, pp. 1-15, Mar. 2021.
- [93] X. Yuan, P. Savarese, and M. Maire, "Growing efficient deep networks by structured continuous sparsification," *9th Int. Conf. Learn. Represent.*, 2021, Online, pp: 1-18.
- [94] X. Zhou, W. Zhong, Z. Chen, S. Diao, and T. Zhang, "Efficient Neural Network Training via Forward and Backward Propagation Sparsification," *Adv. Neural Inf. Process. Syst.*, vol. 34, pp: 15216-15229, 2021.
- [95] Y. He, P. Liu, Z. Wang, Z. Hu, and Y. Yang. "Filter pruning via geometric median for deep convolutional neural networks acceleration," in *Proc. 32nd IEEE/CVF Conf. Comput. Vis. Pattern Recognit.*, 2019, Long Beach, USA, pp: 4340-4349.
- [96] Y. Tang, Y. Wang, Y. Xu, D. Tao, C. X. Xu, C. Xu, and C. Xu, "Scop: Scientific control for reliable neural network pruning," *Adv. Neural Inf. Process. Syst.*, vol. 33, pp: 10936-10947, 2020.